

Spin-sensitive atom mirror via spin-orbit interaction

Lu Zhou^{1,3*}, Ren-Fei Zheng¹ and Weiping Zhang^{2,3}

¹*Department of Physics, School of Physics and Material Science,
East China Normal University, Shanghai 200062, China*

²*Department of Physics and Astronomy, Shanghai Jiaotong University, Shanghai 200240, China and*

³*Collaborative Innovation Center of Extreme Optics,
Shanxi University, Taiyuan, Shanxi 030006, China*

Based on the spin-orbit coupling which have been recently implemented in neutral cold atom gas, here we propose a scheme to realize spin-dependent scattering of cold atoms. In particular we consider a matter wave packet of cold atom gas impinging upon a step potential created by the optical light field, inside which the atoms are subject to spin-orbit interaction. We show that the proposed system can act as a spin polarizer or spin-selective atom mirror for the incident atomic beam. The principle and the operating parameter regime of the system are carefully discussed.

PACS numbers: 03.75.-b, 42.25.Bs, 42.50.Gy

I. INTRODUCTION

Recent years have witnessed rapid development of atom interferometry, which promises wide applications ranging from precision measurement to fundamental quantum mechanics [1]. As one of the key elements in atom interferometry, the technique of atom mirror have been experimentally implemented and greatly improved along with the development of atom optics [2]. The atom mirror was first proposed by Cook and Hill [3], and the very first experiment was carried out in the late 1980s [4], in which the mirror reflection of a thermal atomic beam was implemented. From then on, various kinds of atom mirror have been developed with different purposes. Nowadays typical atom mirror utilize the technique of bragg scattering [5] or evanescent field formed at a dielectric interface.

It is well-known that the polarization of a circularly-polarized light will be reversed upon reflection at normal incidence. From the quantum-mechanical perspective, this is because each circularly-polarized photon is attributed with a spin whose direction is parallel to that of the light propagation [6]. In other words, the spin and center-of-mass motion are attached to each other for circularly-polarized light. The light polarization is an important physical quantity and can be modified during the light propagation, which have many important applications such as polarized glasses.

Pseudo-spin can be constructed from the atomic internal energy level structure, which provides an extra internal degree-of-freedom to the atomic dynamics in analogy to the photon polarization. Only very recently have the atomic spin been successfully attached to its center-of-mass motion via the mechanism of artificial spin-orbit (SO) coupling [7, 8], which also provides a new possibility to develop a spin-sensitive atom mirror. Such an atom mirror can reflect the atomic beam and in the meanwhile

reverse its spin-polarization on demand, which can find interesting applications such as atom interferometry with spin-dependent phase shifts [9].

In this paper we pay special attention to the case of the reflection of atoms impinging upon a potential created by an off-resonant optical light field. The atoms are subject to SO-coupling inside the potential, which is the origin of the spin polarization of the reflected atomic beam. Previously the role of the SO interaction on the tunnelling dynamics had been studied in [10–14]. Our previous work also studied the Goos-Hänchen shifts in spin-orbit-coupled cold atoms upon total-internal-reflection [15]. However the role of SO-coupling on the atomic spin-polarization properties upon reflection has not been explored to our knowledge. In the following we will carefully explore how the atomic populations are distributed among different spin states upon the reflection. By analyzing these results, we discuss how to design an efficient spin-sensitive atom mirror. Since SO-coupling is generated from a non-Abelian gauge potential, we hope that our results can be useful for the design of non-Abelian atom optics elements and atom interferometers which exploit the non-Abelian Aharonov-Bohm effect [16].

The paper is organized as follows: In Sec II we present our model and an analyzation of the atomic scattering properties is presented. Sec III is devoted to the calculation of the spin-polarization rate as well as the reflectivity. Based on that, we discussed the role of the system acting as the spin-sensitive atom mirror. A brief discussion on the case of one-dimensional SO-coupling is given in Sec IV. Finally we conclude in Sec V.

II. MODEL

We consider the following model depicted in Fig. 1: An atomic beam incident upon a potential barrier from the x -direction. The scattering potential is described by $V(x) = V_0\Theta(x)$, where $\Theta(x)$ is the Heaviside step function. Such a step potential can be created via a super-Gaussian laser beam with a large-enough order

*lzhou@phy.ecnu.edu.cn

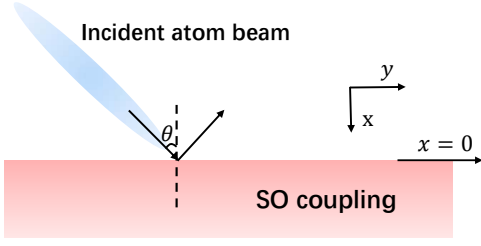


FIG. 1: (Color online) Schematic diagram showing the system under consideration. A beam of cold atoms incident upon a potential barrier with an incident angle θ . As SO-coupling are superimposed inside the barrier, the atoms will subject to spin-dependent scattering.

[17] and width compared to the atomic de-Broglie wavelength. Inside the barrier, atoms are subject to Rashba SO-coupling, which can be generated in neutral cold atoms with a tripod or ring coupling scheme [18–22]. The degree-of-freedom in z -direction is assumed to be frozen out by external confinement, effectively reducing the dynamics to the xy -plane. The effective atomic Hamiltonian inside the potential barrier can then be written as

$$H = \frac{\hbar^2 \mathbf{k}^2}{2m} + \frac{\hbar^2 a}{m} (k_x \sigma_y - k_y \sigma_x) + V_0, \quad (1)$$

where $\mathbf{k}^2 = k_x^2 + k_y^2$, and a , which characterizes the strength of the SO coupling, is taken to be positive with dimension of wavenumber.

The eigenvectors of Hamiltonian (1) split into two branches and can generally be expressed as $|\phi_{\mathbf{k}}^{\pm}\rangle = C e^{i(k_x x + k_y y)} |\chi_{\mathbf{k}}^{\pm}\rangle$ with C the normalization constant and

$$|\chi_{\mathbf{k}}^{\pm}\rangle = \begin{pmatrix} -2a(k_y + ik_x) \\ E_{\mathbf{k}}^{\pm} - V_0 - \mathbf{k}^2 \end{pmatrix}, \quad (2)$$

in which $E_{\mathbf{k}}^{\pm}$ is the corresponding eigenenergy (scaled by $\hbar^2/2m$) satisfying the relation

$$(\mathbf{k}^2 + V_0 - E_{\mathbf{k}})^2 - 4a^2 \mathbf{k}^2 = 0, \quad (3)$$

from which we can get the energy spectrum $E_{\mathbf{k}} = \mathbf{k}^2 \pm 2a|\mathbf{k}| + V_0$.

In the situation considered here, the system is left free along the y -direction and semi-infinite in the x -direction, thus k_y is real and k_x is generally complex. As those had been illustrated in Ref. [11], the eigenfunctions of the system can be grouped into three categories according to their properties: (i) propagating states with k_x real, (ii) evanescent states (only exist near the boundary of the system and propagate along it) with $k_x = i\kappa$ (requiring $|\kappa| < |k_y|$) and (iii) oscillating evanescent states with $k_x = K'_x + iK''_x$.

In order to better understand the properties of these eigenstates, we plot in Fig. 2 the energy spectra ($E_{\mathbf{k}} - V_0$) as a function of $|k_x|$ for two typical values of k_y , which

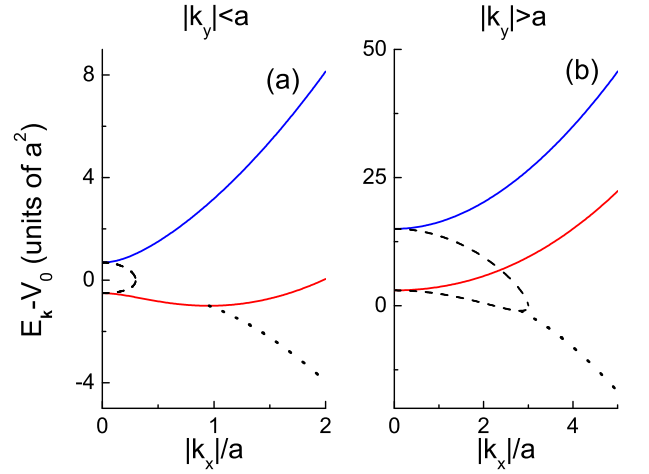


FIG. 2: (Color online) Typical energy spectra of the different states described by $E_{\mathbf{k}} = \mathbf{k}^2 \pm 2a|\mathbf{k}| + V_0$. The solid (blue and red) lines correspond to the up and down branches of the propagating states. The black dashed line represents the evanescent states while the black dotted line is for the oscillating evanescent states. (a) $|k_y| < a$; (b) $|k_y| > a$.

exhibit different structures depending on the value of k_y . For both cases, the two branches of propagating states are separated by a gap of $4a|k_y|$ at $|k_x| = 0$. When $|k_y| < a$, $|k_x| = \sqrt{a^2 - k_y^2}$ is the energy minimum of the lower propagating branch and the dispersion curve of the evanescent states forms a lobe with its tip located at $|k_x| = |k_y|$, which intersects with the energy spectra of propagating states at $|k_x| = 0$. While for $|k_y| > a$, $|k_x| = 0$ becomes the energy minimum of the lower propagating branch, which intersects with the evanescent lobe at some finite $|k_x|$ besides $|k_x| = 0$. The oscillating evanescent states possess minimum energies among these three types of solutions for both cases, and are linked to the energy minimum of the lower propagating branch for $|k_y| < a$ and the evanescent lobe for $|k_y| > a$.

A wide range of the atomic incident energy and incident angle will be considered in the following discussion to include all three branches of the atomic dispersion spectrum, under which circumstance the incident atom beam will undergo either total internal reflection or partial reflection. We take all these situations into account in order to find out the conditions under which the spin-polarized reflection of atoms can be realized with high efficiency.

We assume that the atoms are initially prepared in the spin- s ($s = \uparrow, \downarrow$) propagating states with energy $E_{in} = k_x^2 + k_y^2$ and incident upon the step potential from $x < 0$, then in the left region ($x < 0$) the wavefunction reads

$$|\psi_{\mathbf{k},s}^{(L)}\rangle = e^{i(k_x x + k_y y)} |s\rangle + e^{i(-k_x x + k_y y)} \sum_{s'} r_{ss'} |s'\rangle, \quad (4)$$

in which $r_{ss'}$ are reflection amplitudes.

From Fig. 2 one can see that any equal-energy surface has two intersections with the dispersion curve (in-

cluding that of oscillating evanescent eigenstates since $k_x = \pm K'_x + iK''_x$, which indicate that the atom propagates inside the barrier in the form of linear superpositions of two of the eigenfunctions described above. Depending on the properties of the two eigenstates, the atom mirror operate in the following four regimes:

(i) Two propagating states (2P). There exist two different cases in this regime: One eigenstate is in the upper dispersion branch while the other one is in the lower branch, or both eigenstates are in the lower dispersion branch. For the first case the wavefunction in the right region ($x > 0$) is

$$\left| \psi_{\mathbf{k}}^{(2P)} \right\rangle = b_1 e^{i(k_{x1}x + k_y y)} \left| \chi_{\mathbf{k}1}^+ \right\rangle + b_2 e^{i(k_{x2}x + k_y y)} \left| \chi_{\mathbf{k}2}^- \right\rangle, \quad (5)$$

with the modulus of the wave vector $|\mathbf{k}_1| = -a + \sqrt{a^2 + E_{in} - V_0}$ and $|\mathbf{k}_2| = a + \sqrt{a^2 + E_{in} - V_0}$. For the case of the two propagating eigenstates both in the lower dispersion branch, which can only occur when $|k_y| < a$ as shown in Fig. 2(a), one has negative $\partial E_k / \partial k_x$ which means that the wave points outwards from the barrier while the other one with positive $\partial E_k / \partial k_x$ propagate inwards through the barrier. The corresponding wavefunction reads

$$\left| \psi_{\mathbf{k}}^{(2P)} \right\rangle = b_1 e^{i(-k_{x1}x + k_y y)} \left| \chi_{\mathbf{k}1}^+ \right\rangle + b_2 e^{i(k_{x2}x + k_y y)} \left| \chi_{\mathbf{k}2}^- \right\rangle, \quad (6)$$

with $|\mathbf{k}_1| = a - \sqrt{a^2 + E_{in} - V_0}$ and $|\mathbf{k}_2|$ kept unchanged.

(ii) One propagating state and one evanescent state (1P1E). When $|\mathbf{k}_1| < |k_y|$ one wave becomes evanescent and the wavefunction is

$$\left| \psi_{\mathbf{k}}^{(1P1E)} \right\rangle = b_1 e^{-\kappa_1 x + i k_y y} \left| \chi_{\mathbf{k}1}^+ \right\rangle + b_2 e^{i(k_{x2}x + k_y y)} \left| \chi_{\mathbf{k}2}^- \right\rangle, \quad (7)$$

with $\kappa_1 = \sqrt{k_y^2 - |\mathbf{k}_1|^2}$.

(iii) Two evanescent states (2E). When $|\mathbf{k}_2| < |k_y|$ both waves are evanescent with the wavefunction

$$\left| \psi_{\mathbf{k}}^{(2E)} \right\rangle = b_1 e^{-\kappa_1 x + i k_y y} \left| \chi_{\mathbf{k}1}^+ \right\rangle + b_2 e^{-\kappa_2 x + i k_y y} \left| \chi_{\mathbf{k}2}^- \right\rangle, \quad (8)$$

with $\kappa_2 = \sqrt{k_y^2 - |\mathbf{k}_2|^2}$.

(iv) Two oscillating evanescent states (2OE). When $V_0 > a^2 + E_{in}$ inside the barrier the atoms propagate with the wavevector $k_x = K'_x + iK''_x$ with K'_x, K''_x satisfy $K_x'^2 K_x''^2 = a^2 (V_0 - E_{in} - a^2)$ and $K_x'^2 - K_x''^2 = 2a^2 + E_{in} - V_0 - k_y^2$. The wavefunction then reads

$$\left| \psi_{\mathbf{k}}^{(2E)} \right\rangle = e^{-K_x'' x + i k_y y} \left[b_1 e^{i K_x' x} \begin{pmatrix} a(iK_x' - K_x'' + k_y) \\ a^2 + iK_x' K_x'' \end{pmatrix} + b_2 e^{-i K_x' x} \begin{pmatrix} a(-iK_x' - K_x'' + k_y) \\ a^2 - iK_x' K_x'' \end{pmatrix} \right], \quad (9)$$

By integrating the Schrödinger equation $H\psi(x) = E\psi(x)$ over the interval expanded around the interface $x = 0$, one can have

$$-\frac{\partial \psi}{\partial x} + ia\sigma_y \psi|_{0^+} = -\frac{\partial \psi}{\partial x}|_{0^-}. \quad (10)$$

The reflection amplitudes $r_{ss'}$ can be determined from Eq. (10) together with the continuous boundary condition. Due to the symmetry inherent in the system, one can verify that $r_{\uparrow\uparrow}(k_x, k_y) = r_{\downarrow\downarrow}(k_x, -k_y)$ and $r_{\uparrow\downarrow}(k_x, k_y) = -r_{\downarrow\uparrow}(k_x, -k_y)$.

In the above analysis a sharp interface at $x = 0$ is assumed to separate the regions with and without the SO-interaction. This will require highly focused dressing laser beam. In practical experiment a nonuniform SO-coupling strength $a(x)$ with its interface extend over finite width d would be much easier to generate. A strict treatment on the case of general interface will resort to time-dependent numerical simulation of the scattering dynamics, which will be left for further investigation and not discussed here. However we would like to note that, similar to the previous study on electron scattering [12], the essential physics derived here for the case of sharp interface will be preserved for the case of a smooth adiabatic interface $\lambda/d \ll 1$ ($\lambda = 2\pi/|\mathbf{k}|$ characterize the atom wavelength). For a smooth interface $a(x)$ changes slowly on the scale of the atom wavelength and the atomic spin will adjust itself adiabatically to the momentum when travelling through it. The main physics of spin scattering will not be undermined with the simplified treatment of a sharp interface.

III. RESULTS AND DISCUSSION

Two physical quantities are at the core of the proposed spin-sensitive atom mirror: Reflectivity and spin-polarization efficiency. For the present setup, the spin-dependent reflectivity is defined as $r_s = \sum_{s'} |r_{ss'}|^2$. The reflected particle current in the longitudinal (x)-direction is $J_s(k_x, k_y) = -\frac{\hbar k_x}{m} \sum_{s'} |r_{ss'}|^2$, while that for the spin current, we follow the definition suggested by Shi *et al.*, [23]

$$J_s^j(k_x, k_y) = \langle v_x \sigma_j \rangle = -\frac{\hbar k_x}{m} \begin{pmatrix} 2 \operatorname{Re}(r_{ss} r_{ss'}^*) \\ -2 \operatorname{Im}(r_{ss} r_{ss'}^*) \\ |r_{ss}|^2 - |r_{ss'}|^2 \end{pmatrix}. \quad (11)$$

The efficiency of spin polarization upon reflection is characterized by the ratio of the spin current to the particle current: $P_s^j = J_s^j / J_s$. Here we concentrate on the spin- z component of the reflected current, and the spin polarization rate upon reflection is characterized by the quantity P_s , which is defined as

$$P_s = (1 - J_s^z / J_s) / 2. \quad (12)$$

If the spin of the atom completely flips upon reflection, $P_s = 1$; Otherwise if the atomic spin does not flip at all, $P_s = 0$.

We calculate r_s and P_s as functions of incident angle and SO-coupling strength a with the atomic incident energy E_{in} fixed. The potential barrier height are set as

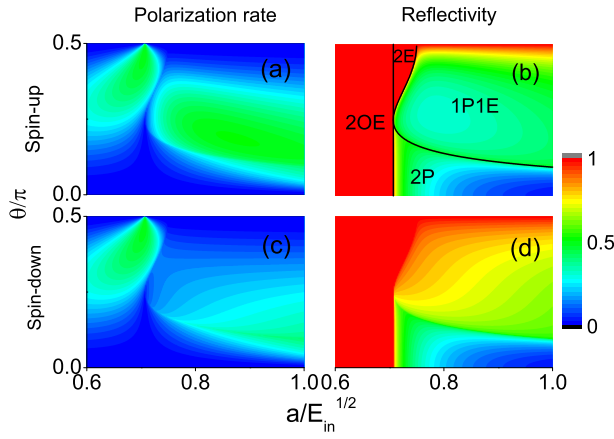


FIG. 3: (Color online) The contour plot of the spin-polarization efficiency and reflectivity versus the incident angle and the SO-coupling strength $a/\sqrt{E_{in}}$. The potential barrier $V_0 = 1.5E_{in}$. (a) and (b) are for the incident atoms prepared in the spin-up hyperfine state; while (c) and (d) are for the spin-down. The four parameter regimes discussed in the text are labeled in (b), which are the same for the other three subplots.

$V_0 = 1.5E_{in}$. The results are shown in Fig. 3. Both the case of initially incident spin-up and down atoms are considered. The four regimes referred above can be clearly observed (also indicated in Fig. 3(b)):

(i) When the SO-coupling strength is relatively small, i.e., $a < \sqrt{V_0 - E_{in}}$, inside the barrier the atomic beam can only exist in the form of oscillating evanescent wave (2OE) and hence it experiences total internal reflection. This means that the atom mirror will have the property of omni-reflection, i.e., atoms with any incident angle will be reflected. As shown in Fig. 3 (a) and (c), in this regime various spin-polarization rate can be achieved via adjusting the incident angle θ , and one can reach high polarization rate (approximately up to 0.5) for large incident angle, which is ideal for a spin-selective atom mirror setup.

(ii) In a small parameter region of $a > \sqrt{V_0 - E_{in}}$, when the atomic incident angle exceeds the critical value $\theta_c \equiv \sin^{-1} [(a + \sqrt{a^2 + E_{in} - V_0})/\sqrt{E_{in}}]$, total internal reflection can still take place, in this case only evanescent wave solutions exist inside the barrier (2E). Similar to the previous case, the atom mirror can also operate in this regime with high efficiency and high polarization rate can be achieved.

(iii) With the increase of SO-coupling strength a , one enters into the 2P regime when the incident angle θ is relatively small ($\theta < \sin^{-1} [(a - \sqrt{a^2 + E_{in} - V_0})/\sqrt{E_{in}}]$). In this parameter region, most incident atoms will propagate through the barrier in the form of propagating waves, which lead to very low reflectivity.

(iv) In other regions of $a > \sqrt{V_0 - E_{in}}$, one enters into the 1P1E regime in which one propagating wave solution and one evanescent wave solution exist inside the barrier. In this regime part of the atoms propagate inside the barrier and will not be reflected. The polarization rate

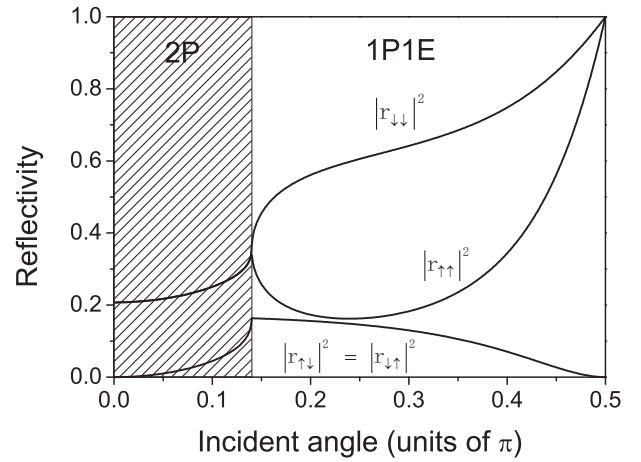


FIG. 4: Reflectivity versus incident angle. The parameters are set as $a/\sqrt{E_{in}} = 0.8$ and $V_0 = 1.5E_{in}$. Inside the shadow area the atoms propagate inside the barrier in the form of two propagating states (2P), while in the rest area one have one propagating state and one evanescent state (1P1E) inside the barrier.

will be accordingly varied with the incident angle, and the maximum value of 0.5 can also be achieved.

By comparing the spin-polarization rate and reflectivity in Fig. 3 for incident spin-up and spin-down atoms, one can notice that they are identical except in the 1P1E regime. More specifically, we have $|r_{\downarrow\downarrow}|^2 = |r_{\uparrow\uparrow}|^2$ with $|r_{\uparrow\downarrow}|^2 \neq |r_{\downarrow\uparrow}|^2$ in this regime. The results are shown in Fig. 4. So in this parameter region the spin of reflected atoms can be effectively polarized for an incident atom beam with equal spin-up and spin-down populations.

We would like to note that under the present setup, for normal incidence ($\theta = 0$), no spin polarization takes place. The spin-polarization efficiency is also very low for small incident angle. This restricts the working threshold of the atom mirror acting as a spin polarizer. However this provides new possibilities for the realization of spin filter or spin-selective atom mirror. For example, suppose that a mixture of spin- \uparrow and \downarrow atoms incident upon the atom mirror at relatively small incident angle (approaching normal incidence), and by applying a homogeneous magnetic field along the z -direction one can induce a Zeeman energy splitting between the atomic magnetic sub-levels. In this case the essential physics inherent in the dispersion curve displayed in Fig. 2 would not be altered, however the incident energy of spin- \uparrow and \downarrow atoms will be different. By appropriately tuning the Zeeman energy splitting one can have, for example, spin- \uparrow atoms in the 2OE regime while the spin- \downarrow ones are in the 2P regime. As a result only the spin- \uparrow atoms will be reflected and the spin- \downarrow ones will penetrate through the potential and the spin-selective reflection can then be realized. The quantum-state-selective mirror reflection of atoms have been studied before in [24], in which the evanescent field formed at a dielectric interface serves as the atom mirror. Here we provide a new scheme to construct this special atom optical element.

IV. CASE OF EQUAL RASHBA-DRESSSELHAUS SPIN-ORBIT INTERACTION

The very first SO-interaction implemented in neutral cold atoms is of one-dimensional equal Rashba-Dresselhaus type [8], so here we briefly address the case of replacing the Rashba SO-interaction in our model by the one-dimensional one. First consider the case that the Hamiltonian inside the potential barrier is

$$H = \frac{\hbar^2 \mathbf{k}^2}{2m} + \frac{\hbar^2 a}{m} k_y \sigma_x + V_0. \quad (13)$$

The dispersion equation then becomes

$$(\mathbf{k}^2 + V_0 - E_k)^2 - 4a^2 k_y^2 = 0. \quad (14)$$

A direct result of the dispersion relation (14) is that it does not support oscillating evanescent eigenstate solutions. In addition to that, in contrast to Eq. (10) the SO-coupling $k_y \sigma_x$ have no contribution to the boundary condition in the x -direction. As a result, the reflection properties of the system change qualitatively. The results are shown in Fig. 5.

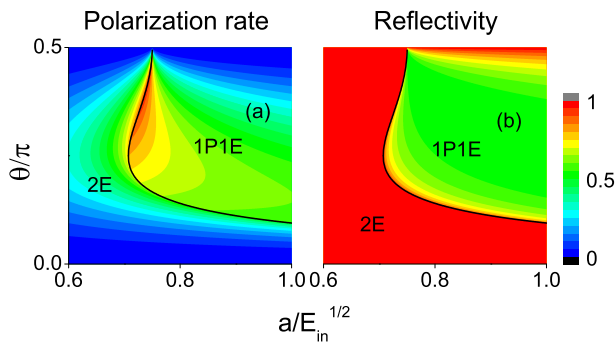


FIG. 5: (Color online) Same as Fig. 3 except that the SO-coupling term have been replaced by $k_y \sigma_x$. The results are identical for incident spin- \uparrow and \downarrow atoms. The black line separates the regime of 2E and 1P1E.

For the parameters chosen here ($V_0 > E_{in}$), one cannot enter into the 2P regime. It is interesting to note that on the boundary which separates the regime of 2E and 1P1E, maximum polarization rate ($P \approx 1$) can be achieved.

Finally, we comment on the case for which the SO-coupling term is proportional to $k_x \sigma_y$, we found out that evanescent solutions will be absent and atomic spin cannot be polarized upon reflection.

V. SUMMARY

In summary, we have studied the possibility of creating a spin-sensitive atom mirror via SO-coupling. The spin polarization rate and reflectivity are calculated as a function of incident energy, incident angle as well as the SO-coupling strength. Depending on these parameters, incident atoms will be subject to quite different scattering processes. We carefully analyzed these results and showed that the atom mirror can effectively polarize the atomic spin upon reflection. Due to the rich spin-dependent scattering properties inherent in this system, the atom mirror can also perform spin-selective reflection. These properties can find applications in the spin-dependent atom interferometer and quantum measurement. In experiment, one can expect that the predicted effect can be readily measured from the density evolution of the atomic ensemble via absorption imaging [25].

Acknowledgments

We thank Han Pu for careful reading and many useful comments on the manuscript. This work is supported by National Key Research Program of China under Grant No. 2016YFA0302000 and Grant No. 2011CB921604, National Natural Science Foundation of China under Grant No. 11374003.

-
- [1] See P. R. Berman, editor. *Atom Interferometry* (Academic Press, San Diego, 1997); A. D. Cronin, J. Schmiedmayer, and David E. Pritchard, *Rev. Mod. Phys.* **81**, 1051 (2009), and references therein.
- [2] C. S. Adams, M. Sigel, and J. Mlynek, *Phys. Rep.* **240**, 143 (1994); P. Meystre, *Atom Optics* (Springer-Verlag, New York, 2001).
- [3] R. J. Cook and R. K. Hill, *Opt. Commun.* **43**, 258 (1982).
- [4] V. I. Balykin, V. S. Letokhov, Yu. B. Ovchinnikov, and A. I. Sidorov, *Pis'ma Zh. Eksp. Teor. Fiz.* **45**, 282 (1987) [*JETP Lett.* **45**, 353 (1987)].
- [5] P. J. Martin, B. G. Oldaker, A. H. Miklich, and D. E. Pritchard, *Phys. Rev. Lett.* **60**, 515 (1988); D. M. Giltner, R. W. McGowan, and S. A. Lee, *Phys. Rev. Lett.* **75**, 2638 (1995); G. Birkl, M. Gatzke, I. H. Deutsch, S. L. Rolston, and W. D. Phillips, *Phys. Rev. Lett.* **75**, 2823 (1995).
- [6] R. A. Beth, *Phys. Rev.* **50**, 115 (1936).
- [7] J. Dalibard, F. Gerbier, G. Juzeliūnas, and P. Öhberg, *Rev. Mod. Phys.* **83**, 1523 (2011); N. Goldman, G. Juzeliūnas, P. Öhberg, I. B. Spielman, *Rep. Prog. Phys.* **77**, 126401 (2014); H. Zhai, *Rep. Prog. Phys.* **78**, 026001 (2015).
- [8] Y.-J. Lin, K. Jiménez-García and I. B. Spielman, *Nature* **471**, 83 (2011). P. Wang, Z.-Q. Yu, Z. Fu, J. Miao, L. Huang, S. Chai, H. Zhai, and J. Zhang, *Phys. Rev. Lett.* **109**, 095301 (2012). L. W. Cheuk, A. T. Sommer, Z. Hadzibabic, T. Yefsah, W. S. Bakr, and M. W. Zwierlein, *Phys. Rev. Lett.* **109**, 095302 (2012). J.-Y. Zhang, S.-C. Ji, Z. Chen, L. Zhang, Z.-D. Du, B. Yan, G.-S. Pan, B.

- Zhao, Y.-J. Deng, H. Zhai, S. Chen, and J.-W. Pan, *Phys. Rev. Lett.* **109**, 115301 (2012).
- [9] R. Trubko, J. Greenberg, M. T. St. Germaine, M. D. Greigore, W. F. Holmgren, I. Hromada, and A. D. Cronin, *Phys. Rev. Lett.* **114**, 140404 (2015).
- [10] G. Juzeliūnas, J. Ruseckas, A. Jacob, L. Santos, and P. Öhberg, *Phys. Rev. Lett.* **100**, 200405 (2008). G. Juzeliūnas, J. Ruseckas, and J. Dalibard, *Phys. Rev. A* **81**, 053403 (2010).
- [11] V. A. Sablikov and Y. Y. Tkach, *Phys. Rev. B* **76**, 245321 (2007).
- [12] M. Khodas, A. Shekhter, and A. M. Finkel'stein, *Phys. Rev. Lett.* **92**, 086602 (2004).
- [13] Y. Ban and E. Y. Sherman, *Phys. Rev. A* **85**, 052130 (2012).
- [14] D.-W. Zhang, Z.-Y. Xue, H. Yan, Z. D. Wang, and S.-L. Zhu, *Phys. Rev. A* **85**, 013628 (2012).
- [15] L. Zhou, J.-L. Qin, Z. Lan, G. Dong, and W. Zhang, *Phys. Rev. A* **91**, 031603 (R) (2015).
- [16] K. Osterloh, M. Baig, L. Santos, P. Zoller, and M. Lewenstein, *Phys. Rev. Lett.* **95**, 010403 (2005); A. Jacob, P. Öhberg, G. Juzeliūnas, and L. Santos, *Appl. Phys. B* **89**, 439 (2007).
- [17] G. Dong, S. Edvardsson, W. Lu, and P. F. Barker, *Phys. Rev. A* **72**, 031605(R) (2005); J. S. Liu and M. R. Taghizadeh, *Opt. Lett.* **27**, 1463 (2002).
- [18] Y. Zhang, L. Mao, and C. Zhang, *Phys. Rev. Lett.* **108**, 035302 (2012).
- [19] G. Juzeliūnas, J. Ruseckas, M. Lindberg, L. Santos, and P. Öhberg, *Phys. Rev. A* **77**, 011802(R) (2008).
- [20] C. Zhang, *Phys. Rev. A* **82**, 021607(R) (2010).
- [21] D. L. Campbell, G. Juzeliūnas, and I. B. Spielman, *Phys. Rev. A* **84**, 025602 (2011).
- [22] L. Huang, Z. Meng, P. Wang, P. Peng, S.-L. Zhang, L. Chen, D. Li, Q. Zhou, and J. Zhang, *Nat. Phys.* **12**, 540 (2016).
- [23] J. Shi, P. Zhang, D. Xiao, and Q. Niu, *Phys. Rev. Lett.* **96**, 076604 (2006).
- [24] V. I. Balykin, V. S. Letokhov, Yu. B. Ovchinnikov, and A. I. Sidorov, *Phys. Rev. Lett.* **60**, 2137 (1988). W. Zhang and D. F. Walls, *Phys. Rev. Lett.* **68**, 3287 (1992).
- [25] L. Khaykovich, F. Schreck, G. Ferrari, T. Bourdel, J. Cubizolles, L. D. Carr, Y. Castin, C. Salomon, *Science* **296**, 1290 (2002).